Published in final edited form as:
Exp Cell Res. 2011 April 1; 317(6): 823–837. doi:10.1016/j.yexcr.2010.12.008.

Annexin A6 contributes to the invasiveness of breast carcinoma cells by influencing the organization and localization of functional focal adhesions

Amos M. Sakwe[a,*], **Rainelli Koumangoye**[a], **Bobby Guillory**[a], and **Josiah Ochieng**[a,b,c]

[a] Department of Biochemistry and Cancer Biology, Meharry Medical College, Nashville TN, 37208 USA.

[b] Center for Aids Health Disparity Research, Meharry Medical College, Nashville, TN, 37208 USA

[c] Department of Cancer Biology, Vanderbilt University, Nashville, TN, USA

Abstract

The interaction of annexin A6 (AnxA6) with membrane phospholipids and either specific extracellular matrix (ECM) components or F-actin suggests that it may influence cellular processes associated with rapid plasma membrane reorganization such as cell adhesion and motility. Here, we examined the putative roles of AnxA6 in adhesion-related cellular processes that contribute to breast cancer progression. We show that breast cancer cells secrete annexins via the exosomal pathway and that the secreted annexins are predominantly cell surface-associated. Depletion of AnxA6 in the invasive BT-549 breast cancer cells is accompanied by enhanced anchorage-independent cell growth but cell-cell cohesion, cell adhesion/spreading onto collagen type IV or fetuin-A, cell motility and invasiveness were strongly inhibited. To explain the loss in adhesion/motility, we show that vinculin-based focal adhesions in the AnxA6-depleted BT-549 cells are elongated and randomly distributed. These focal contacts are also functionally defective because the activation of focal adhesion kinase and the phosphoinositide-3 kinase/Akt pathway were strongly inhibited while the MAP kinase pathway remained constitutively active. Compared with normal human breast tissues, reduced AnxA6 expression in breast carcinoma tissues correlates with enhanced cell proliferation. Together this suggests that reduced AnxA6 expression contributes to breast cancer progression by promoting the loss of functional cell-cell and/or cell-ECM contacts and anchorage-independent cell proliferation.

Introduction

Several steps in the multistep process of cancer metastasis require efficient cell-cell and cell-extracellular matrix (ECM) interactions. These interactions in turn promote the invasion of the parenchyma of surrounding tissues and of distant organs by invasive/metastatic tumor cells [1]. At the center of this behavior of invasive cancer cells is the formation of mature and functional adhesion plaques at sites of cell contact with the ECM and/or adherens

* Corresponding author: Amos M. Sakwe, Department of Biochemistry and Cancer Biology, Meharry Medical College, Nashville TN, 37208 USA. Tel: 1-615-327-6064; Fax: 1-615-327-6442; asakwe@mmc.edu.

junctions between the tumor cells on one hand and on the other hand, between normal and tumor cells. Adhesion plaques and adherens junctions are stabilized by the highly dynamic actin cytoskeleton that in turn is modulated by a large number of actin binding proteins [2]. Amongst these proteins are members of the annexin family of Ca^{2+}-dependent phospholipid binding proteins [3].

Annexins Ca^{2+}-dependently interact with distinct plasma membrane regions to promote membrane segregation and each annexin family member requires a different Ca^{2+} concentration for its translocation to the membrane [4,5]. Although their precise functions remain unclear, their Ca^{2+} responsiveness and membrane binding properties, suggests that annexins may link Ca^{2+} signaling with actin dynamics at membrane contact sites [3,6]. Available evidence nevertheless reveal that annexins regulate a multitude of signaling pathways that promote cell proliferation, cell motility, tumor invasion and metastasis, angiogenesis, apoptosis and drug resistance via distinct mechanisms [3,7,8].

Annexin A6 (AnxA6) is an unusual member of the annexin family in that it contains eight rather than four annexin repeats [9]. Consequently, it has been shown to interact with biological membranes with slightly different kinetics compared with other members of the family [10]. In a recent study, constitutive plasma membrane targeting of AnxA6 not only stabilized the cortical actin cytoskeleton but also inhibited store-operated Ca^{2+} influx and cell proliferation [11]. In support of these observations, ectopic expression of AnxA6 in the AnxA6-null A431 squamous epithelial carcinoma cells reduced their proliferation [12]. Other studies have also shown that AnxA6 is down-regulated in chronic myeloid leukemia [13] and as melanomas progress from a benign to a more malignant phenotype [14]. Meanwhile, depletion of AnxA6 in MDA-MB-436 invasive breast cancer cells led to increased anchorage-independent cell proliferation [15]. Together this suggests that in breast cancer AnxA6 may not only act as a tumor suppressor but also as a cell adhesion/motility promoting factor.

In the present study we examined the involvement of AnxA6 in adhesion-related cellular processes that contribute to breast cancer progression. We demonstrate that AnxA6 expression correlates with the invasive phenotype of breast cancer and that depletion of this protein in the invasive BT-549 breast cancer cells inhibited cellular adhesion, motility and invasiveness. We also show that that the enhanced anchorage-independent proliferation of BT-549 cells following AnxA6 depletion requires sustained MAP kinase activation, while the loss of invasiveness of AnxA6-depleted BT-549 cells may be attributed to its role in the formation of functional focal contacts at appropriate plasma membrane locations and that this is driven by the activation of the phosphoinositide-3 (PI3) kinase/Akt pathway. These data suggest that reduced AnxA6 expression contributes to breast cancer progression by promoting the loss of functional cell-cell and/or cell-ECM contacts and anchorage-independent cell proliferation.

Materials and Methods

Materials

Polyclonal antibodies to AnxA2, AnxA4, AnxA6 as well as phospho-focal adhesion kinase (p-Y397) were purchased from Santa Cruz Biotechnology Inc. (Santa Cruz, CA, USA). Polyclonal antibodies to E-cadherin, N-Cadherin, phospho-PKB/Akt (p-S473) and phospho-ERK1/2 were obtained from Cell Signaling Technology Inc. (Danvers, MA, USA). Monoclonal antibodies to ERK2 as well as HRP, FITC or Texas red-conjugated secondary antibodies were also purchased from Santa Cruz Biotechnology Inc., (Santa Cruz, CA USA). Monoclonal antibody to β-actin and vinculin, were obtained from Sigma (St Louis, MO, USA). Formalin-fixed, paraffin-embedded thin sections of normal human breast and

breast cancer tissues were purchased from Biomax-US (Rockville, MD, USA). Except otherwise indicated cell culture reagents were purchased from Invitrogen or Sigma.

Cell lines and cell culture

The breast cancer cell lines BT-549, MDA-MB-231, MCF-7 and MCF-10A were purchased from ATCC (Manassas, VA, USA). A sub-clone of BT-549 cells stably over-expressing Galectin-3 (clone 11-9-1-4) herein designated BT-Gal3, was a gift from Dr. Avraham Raz (Karmanos Cancer Institute, Wayne State University, Detroit, MI, USA). These cell lines were propagated in Dulbecco's modified Eagle's nutrient F12 (DMEM/F12) medium supplemented with 10% heat-inactivated fetal bovine serum, L-glutamine (2 mM), penicillin (100 units/ml), and streptomycin (50 units/ml) in a 95% air and 5% CO_2 incubator at 37 °C. Human mammary epithelial cells (HuMEC) were kindly provided by Dr. Jennifer Pietenpol (Vanderbilt-Ingram Cancer Center, Vanderbilt Medical Center, Nashville, TN) and were cultured in complete HuMEC Medium (Invitrogen, Carlsbad, CA). The hepatocellular carcinoma cell line HepG2 was obtained from ATCC and maintained in MEM supplemented with 10% heat-inactivated fetal bovine serum, L-glutamine (2 mM), penicillin (100 units/ml), and streptomycin (50 units/ml). The media were changed every 2 to 3 days and except otherwise indicated, cells were sub-cultured by treatment with 0.25% trypsin/ 0.53 mM EDTA solution (Invitrogen, Carlsbad, CA).

RNAi

Sub-confluent BT-549 cells (1×10^5 cells/well) seeded in six-well plates were transfected with 4 μg/well of purified AnxA6-targeted short hairpin RNA (shRNA) in plasmid pSM2c (Open Biosystems, Huntsville, AL) by using Fugene6 reagent as recommended by the manufacturer (Roche Biochemicals). The sequences of the targeted sense region are A6A 5'-CACTCGGACCAATGCTGA-3' and A6B 5'-GACCTCATTGCTGATTTAA-3'. Puromycin (2.5μg/ml) surviving clones were isolated and propagated in selection medium (complete DMEM/F12 containing 2.0 μg/ml puromycin) as long as the cells were in culture. AnxA6 down regulation in the stable BT-549 clones was verified by western blotting and immunofluorescence using polyclonal antibodies to AnxA6.

Isolation of secreted and surface-associated proteins

Cells were cultured until they attained 70-80% confluence. These were then harvested by trypsinization, washed twice in HBSS (Hepes-buffered saline: 11 mM Hepes, 137 mM NaCl, 4 mM KCl, 1 mM glucose) and equal numbers incubated in HBSS with or without 2 mM Ca^{2+} for two hrs at 37 °C. The cells were harvested by centrifugation at 500 × g for 4 min and the culture supernatants (CS) containing total secreted proteins were transferred to new tubes. These were cleared of any cells by centrifugation at 10,000 × g for 10 min at 4 °C. The final supernatant containing the secreted proteins was concentrated by ultrafiltration using the Millipore MCO-3,000 ultrafiltration unit and equal volumes of the extracts used for analysis.

EGTA-elution of surface associated proteins was performed as previously described [16]. Briefly, cells pretreated with or without Ca^{2+} as above were washed once with HBSS and incubated with HBSS containing 10 mM EGTA for 30 min at 4 °C with occasional shaking. The cells were once again harvested by centrifugation at 500 × g for 4 min and the supernatant containing EGTA-solubilized surface-associated proteins (SAP) was cleared by centrifugation at 10,000 × g for 10 min at 4 °C. These were analyzed alongside total cell lysates and the secreted proteins.

Cell fractionation

Total cellular proteins were prepared by resuspending cells in ice-cold RIPA buffer (50 mM Tris-HCl, pH 7.4, 1% NP-40, 0.1% sodium deoxycholate, 150 mM NaCl, 1 mM EDTA), supplemented with protease inhibitor cocktail (Sigma) and incubation on ice for 30 min. The lysates were cleared by centrifugation at 10,000 × g for 10 min at 4 °C. For the preparation of cytosolic and membrane-enriched cellular fractions, cells were resuspended in hypotonic lysis buffer (10 mM HEPES pH 7.9, 10 mM KCl, 1.5 mM $MgCl_2$, 0.34 M sucrose, 10% glycerol, 1 mM dithiothreitol, 1 mM phenylmethylsulfonyl fluoride, and protease inhibitor cocktail (Sigma), homogenized by passage six times through 26G needle and incubated on ice for 30 min. The homogenates were centrifuged at 2,300 × g for 4 min at 4 °C to separate the nuclei from the post nuclear supernatants. The post nuclear supernatants were in turn centrifuged at 100,000 × g for 1 h at 4 °C using the Sorvall M150 micro-ultracentrifuge and S120-AT2 rotor. The resulting supernatants comprising cytosolic proteins were transferred to new tubes while the pellets (membrane-enriched faction) were extracted in ice-cold RIPA buffer for 30 min on ice. After centrifugation at 10,000 × g for 10 min at 4 °C, the supernatant containing the solubilized membrane proteins was transferred to new tubes. The protein content of total cellular proteins or various fractions was determined using the Bradford reagent (Bio-Rad Laboratories) and equal amounts of proteins used for protein electrophoresis and immunoblotting as previously described [17].

Immunohistochemistry

Microscope slides containing thin sections of paraffin-embedded formalin fixed normal, mucous adenocarcinoma and invasive ductal carcinoma human breast tissues (US Biomax, Rockville, MD) were deparaffinized in xylene and rehydrated with decreasing graded alcohol. Antigen retrieval was performed in 0.1M sodium citrate pH 6.0 by heating to 95-96 °C for 20 minutes followed by cooling to room temperature. Endogenous peroxidase blocking, incubation with the indicated primary antibodies and peroxidase-conjugated secondary antibodies were performed as described in the Labeled Streptavidin-Biotin HRP kit (DAKO, Carpinteria, CA, USA). The thin sections were subsequently treated with diaminobenzidine substrate and counterstained with hematoxylin for 5 min. Slides were then dehydrated through a graded series of alcohol, cleared in xylene and mounted with cover slips. Images were acquired with a Zeiss Axioscope Microscope. Quantification was performed from four randomly chosen fields using NIH ImageJ software.

Immunofluorescence

Cells were grown on glass cover slips in complete DMEM/F12 overnight at 37 °C. Except otherwise indicated the cells were serum-starved for 24 h by cultivating them in complete DMEM/F12 in which FBS was replaced with 0.1% BSA. The cells were subsequently fixed in -20 °C cold methanol or in 3% paraformaldehyde (PFA) in PBS followed by permeabilization in 0.5% Triton X-100 in PBS for 10 min at room temperature. Cells were washed once with ice-cold HBSS and fixed in 3% PFA in PBS. For observation of adhesion plaques, cells were pretreated with 3% PFA in PBS containing 0.5% Triton X-100 for 2 min followed by fixation in 3% PFA. Cells were then blocked with 3% BSA in PBS, then incubated with first and secondary antibodies as recently described [17]. For detection of surface-associated AnxA6, non permeabilized PFA-fixed cells were probed with monoclonal anti-AnxA6 antibody followed by Texas Red-conjugated anti-mouse antibody. Samples were washed extensively between the treatments and cover slips were mounted with Prolong Gold with DAPI (Invitrogen). F-actin was detected by incubating PFA-fixed and permeabilized cells with rhodamine-labeled phalloidin (Molecular Probes) diluted 1/20 in PBS. Samples were visualized using a Nikon Eclipse TE-2000-E inverted microscope equipped with NIS-Elements AR software (Nikon, Melville, NY, USA).

Cell Proliferation Assays

For anchorage-independent growth, cells were cultured in complete medium in poly(2-hydroxyethyl methacrylate) (poly(Hema))-coated plates were prepared as previously described [18]. For growth curves in 2D cultures, cells were plated into a 96-well flat bed plate at a density of 2×10^3 cells per well in triplicate then incubated for up to 7 days with medium changed every 3 days. At the end of each time point the alamar blue reagent (Invitrogen, Carlsbad, CA, USA) was diluted 1:10 in HBSS supplemented with 1 mM Ca^{2+} and 0.5 mM Mg^{2+}. The culture medium was aspirated and replaced with 100 μl of diluted reagent per well, followed by incubation at 37 °C for 4-6 h. The proliferation and viability of the cells was determined by measuring the absorbance at 570 versus 600 nm.

Cell adhesion/spreading

Wells of 96-well plates were coated in quadruplicate with 0.5 mg/ml Fetuin-A, 0.1 mg/ml of either collagen type I, collagen type IV, laminin or fibronectin overnight at 4 °C. Prior to use in cell attachment/spreading assays, the coating solutions were aspirated and 1×10^4 cells in serum-free DMEM/F12 were added to each well and incubated overnight (16-24 h) at 37 °C. Controls cells were seeded in complete DMEM/F12 or serum-free DMEM/F12. After aspirating the floating cells the attached cells were photographed using DCM200 digital camera equipped with Scopephoto software (ScopeTek, Hangzhou, China) and cell numbers and viability estimated by alamar blue colorimetric assay as described above.

Three-dimensional growth on Matrigel

This was performed as described previously [19]. Briefly, 100 μl of growth factor reduced Matrigel (Becton Dickinson Labware, Bedford, MA, USA) were dispensed into wells of a 96-well microtitre plate and allowed to gel at 37 °C for at least 30 min. Cells were trypsinized, washed and resuspended in complete DMEM/F12 medium and then plated at a density of 5×10^3 cells per well. These were then incubated for up to 10 days with medium changes after every 4 days. The 3-D structures were captured with DCM200 digital camera and Scopephoto software.

Transwell Migration and Invasion Assays

Migration and invasion assays were determined in triplicate using 24-well, 8 μm pore transwell inserts and Matrigel coated transwell invasion chambers respectively, according to the manufacturer's protocol (Becton Dickinson Labware, Bedford, MA, USA). Briefly, cells were harvested by trypsinization, washed twice and resuspended in serum-free DMEM/F12. DMEM/F12 medium containing 10% FBS was then added to the lower chamber as the chemoattractant and 2.5×10^5 cells in 500 μl of serum-free DMEM/F12 were added to the upper insert chamber or on the Matrigel layer. After incubation at 37°C for 24 h the cell suspension in the upper chamber was aspirated and excess Matrigel and/or cells on the insert membrane were removed using a cotton swab. Cells that had migrated through the insert membrane or invaded the Matrigel and insert membrane and reached the lower surface of the filter were subsequently fixed in 3% PFA in PBS, stained with crystal violet and counted under a light microscope. Digital images were captured with DCM200 digital camera and Scopephoto software (ScopeTek, Hangzhou, China). Three random fields were counted for each sample.

Results

Cell surface expression of annexins in breast cancer cells occurs via the exosomal pathway

Previous studies in our laboratory demonstrated that AnxA2, AnxA4 and AnxA6 interact with the abundant serum glycoprotein fetuin-A on the surface of BT-549 breast cancer cells [20]. Since the interaction of annexins with membranes exhibit a high degree of Ca^{2+} sensitivity [4,5] these proteins can be efficiently eluted by EGTA treatment of the intact cells [16]. To test the possibility that other breast cancer cells express and externalize annexins, we treated MCF-7, BT-549, MDA-MB-231 breast cancer cell lines as well as MCF-10A known to retain many characteristics of normal breast epithelial cells [21,22] with EGTA to elute the Ca^{2+}-dependently cell surface-associated proteins (herein denoted SAP). As shown in Fig. 1A, the three breast cancer cell lines express AnxA2, AnxA4 and AnxA6. Surprisingly, MCF-10A cells are AnxA6-null (Fig. 1A, lanes 2 and 6). In the annexin-positive cell lines these proteins are also detected in the EGTA-solubilized SAP extracts. However, the expression levels of AnxA2 and AnxA4 are up-regulated in the AnxA6-depleted BT-549 cells and in the AnxA6-null MCF-10A (Fig. 1A and supplementary Fig. 1A and B).

To show that surface expression of these proteins involves their secretion via the exosomal pathway, BT-549 cells were cultured in HBSS with or without Ca^{2+} for 2 h and the secreted proteins in the culture supernatants (CS) were fractionated into exosome-free (ExF) and exosome-associated (Exos) fractions as recently described [17]. At the end of the treatment the viability of the cells by the Trypan blue exclusion method was at least 98%. To verify that the viability of the cells was not affected by incubation in HBSS or HBSS/EGTA we used a cytotoxicity assay based on secreted lactate dehydrogenase (LDH). As shown in supplementary Fig. S1C and D the basal secretion of LDH by adherent BT-549 cells in complete DMEM/F12 was ~11.5% of total cellular LDH (data not shown). Secretion in HBSS at 37 °C ranged from 8.3-10.1% over the 2 h period and 5.2-7.6% in HBSS/EGTA on ice. Analysis of the secreted fractions, the corresponding SAP extracts and total cellular proteins by immunoblotting revealed that AnxA2 and AnxA6 are Ca^{2+}-dependently secreted by these cells (compare Fig. 1B lanes 4 and 5). The secreted proteins were enriched in the exosomal fractions (Fig. 1B lanes 8 and 9) compared to the exosome-free fractions (Fig. 1B lanes 6 and 7). As expected, Fig. 1B also shows that these proteins were more abundant in the membrane-associated, EGTA-solubilized extracts than in the culture supernatants (Fig. 1B lanes 2 and 3 versus lanes 4 and 5). Finally, as shown in Fig. 1C, AnxA6 is at least 6-fold more abundant on the surface of BT-549 cells than AnxA2. Similar low levels (< 5% of total cellular AnxA2) of cell-surface-associated AnxA2 were also observed in the hepatocellular carcinoma cell line HepG2 (data not shown).

To verify the expression of AnxA6 in BT-549 cells, cells were pretreated with or without 2.0 mM Ca^{2+} and stained with monoclonal antibodies to AnxA6 and co-stained with rhodamine-labeled phalloidin (F-actin) and DAPI (nuclei). As depicted in supplementary Fig. S2, and as expected, AnxA6 co-localized with F-actin. In most of the cells, AnxA6 and actin are concentrated in the plasma membrane with discernible membrane protrusions. The intensity of AnxA6 and F-actin in these membrane protrusions increased with Ca^{2+} concentration (supplementary Fig. S2A, arrows) and may represent early stages of cell adhesion [23]. To demonstrate that a pool of AnxA6 is cell surface-associated, non-permeabilized cells were stained with a monoclonal antibody to AnxA6. This revealed that cell surface-associated AnxA6 is concentrated in the membrane protrusions (Fig. S2B, arrows).

AnxA6 influences growth and adhesion-related properties of BT-549 breast carcinoma cells

Based on the above data, we hypothesized that AnxA6 may influence the adhesion-related properties (cellular adhesion, motility and invasiveness) of invasive breast cancer cells by linking the cell surface to the ECM (extracellular AnxA6) or the plasma membrane to the actin cytoskeleton (intracellular AnxA6). To test this hypothesis, we established stable AnxA6-depleted BT-549 cells by transfecting these cells with shRNA constructs designated A6A and A6B which target distinct regions of AnxA6 coding sequence (ANXA6 transcript variant 1, accession number NM_001155.3). Analysis of the transfected cells by western blotting (Fig. 2A) revealed that depletion of AnxA6 was more efficient in the A6A shRNA transfected cells (herein designated BT-A6A) compared to the A6B shRNA transfected cells (herein designated BT-A6B). The extent of down regulation was >98% in BT-A6A and ~40% in BT-A6B cells compared to the parental or empty vector transfected cells (Fig. 2B). We also show that depletion of AnxA6 in BT-549 cells led to about 2-fold (range 1.5-3 fold) increase in the expression levels of AnxA2 and AnxA4 (Fig. 2A, lane 3). This was confirmed by indirect immunofluorescence using antibodies to these annexin family members (supplementary Fig. 3).

To determine any changes in cell morphology following AnxA6 depletion, parental BT-549, BT-A6A and BT-A6B cells were grown on cell culture plastics in complete medium and examined by phase contract microscopy. As shown in Fig. 2C, compared to the parental BT-549 cells (upper panel), the BT-A6A cells (middle panel) are characteristically spindle-shaped while the BT-A6B cells (lower panel) have characteristically long lamellipodia. This reveals that reduced AnxA6 expression dose dependently altered the morphology of BT-549 cells.

Given the efficient depletion of AnxA6 in the BT-A6A cells these were used in most of the subsequent experiments with the parental BT-549 cells as the control. We first wanted to verify whether AnxA6 is indispensable for anchorage-dependent growth. Parental BT-549 and BT-A6A cells were seeded onto plates coated with or without polyHEMA in complete DMEM/F12 medium and the cell populations observed for up to 48 hrs. As depicted in Fig. 3A, parental BT-549 cells grew as cell masses in anchorage-independent mode while AnxA6-depleted cells proliferated as single cells. In agreement with the growth of AnxA6-depleted MDA-MB-436 breast cancer cells [15], BT-A6A cells continued to proliferate without attaining confluence while the parental cells were confluent by day four (Fig. 3B). This suggests that AnxA6 expression is essential for the formation of cell-cell and cell-ECM contacts and that loss of AnxA6 abolishes contact inhibition and promotes anchorage-independent cell proliferation.

To ascertain that AnxA6-depletion abolished contact inhibition, BT-549 and BT-A6A cells were cultured on fetuin-A or fibronectin coated cover slips and visualized by F-actin staining. Fig. 3C shows that BT-A6A cells grew as clumps on fetuin-A coated cover slips (Fig. 3C, left panel) but surprisingly, these cells attached and spread on fibronectin-coated cover slips (Fig. 3C, right panel). As a consequence of this loss in contact inhibition, BT-A6A cells do not form confluent monolayers and require longer times (16-48h) to attach when cultured in complete medium containing 10% FBS unlike the parental cells. The observed defects in cell adhesion and spreading were however, reversed when BT-A6A cells were cultured in serum-free conditioned medium from the parental BT-549 cells which as shown in Fig. 1 contain AnxA6 (supplementary Fig. S4).

Based on the differential attachment and spreading of BT-A6A cells on either fetuin-A- and fibronectin-coated cover slips (Fig. 3C), we next tested the attachment and spreading of BT-549 and BT-A6A cells on other extracellular matrix components. To do this these cell

lines cells were cultured on fetuin-A, collagen type I, collagen type IV, laminin or Fibronectin-coated tissue culture plastics. Cells grown in serum-free medium (SFM) or complete medium (FBS) were used as controls. As shown in (Fig. 4A, a) and as expected the attachment of parental BT-549 cells in serum-free medium (SFM) was strongly attenuated but they efficiently attached and spread in complete medium (FBS) (Fig. 4A, b and b'). Under similar conditions only about 30% of BT-A6A cells showed signs of spreading (seen as spindle-shaped cells) in complete medium but the cells remained rounded in serum-free medium (Fig. 4A, a'). On fetuin-A-coated plates (FET) and as recently reported [24] BT-549 cells were able to spread albeit less effectively compared to spreading in serum-supplemented medium. On the other hand, the spreading of BT-A6A cells on fetuin-A was virtually abolished (Fig. 4A, c and c'). While adhesion and spreading of either parental BT-549 or BT-A6A cells onto collagen type I (Col I) was less efficient (Fig. 4A, d and d') both cell lines adhered and efficiently spread on fibronectin (Fig. 4A, f and f') and on laminin (data not shown). Interestingly, while BT-549 cells attached and spread on collagen type IV-coated plates (Col IV), BT-A6A cells grown on collagen type IV-coated plates remained mostly rounded (Fig. 4A, e and e'). To verify that these cells were viable even though the AnxA6-depleted cells were rounded and/or loosely attached to the various substrata, the number and viability of the adhering cells were estimated using the alamar blue assay. Fig. 4B confirms that a greater number of BT-549 cells were retained in plates coated with FBS, collagen type IV and fibronectin and that the remaining rounded and/or spindle-shaped, BT-A6A cells were also viable compared with growth in serum-free medium. Together, this suggests that AnxA6 expression in motile/invasive breast cancer cells is necessary for efficient attachment to specific extracellular matrix components.

Reduced expression of AnxA6 inhibits the motility and invasiveness of breast cancer cells

Most invasive breast cancer cells express low levels of E-cadherin and grow in 3D cultures on matrigel as branched or stellate colonies while the weakly invasive or non-invasive cell lines retain E-cadherin expression and grow either as fused colonies or as spherical colonies [22]. In the following assays MCF-10A cells were used as negative control and the galectin-3 expressing BT-549 (BT-Gal3) cells previously shown to be less motile but more invasive than the parental BT-549 cells [25] were used as the positive control. We first examined the expression of AnxA6 and epithelial-mesenchymal markers in these cells by immunoblotting. As shown in Fig. 5A, lane 1, MCF-10A cells are N-cadherin and AnxA6-negative but as expected are E-cadherin positive. While the parental BT-549 and BT-Gal3 cells express similar levels of AnxA6, we consistently detected N-cadherin in BT-A6A cells (Fig. 5A, lane 4). We next tested the ability of BT-A6A cells to grow in 3D cultures in growth factor-reduced matrigel. As shown in Fig. 5B, unlike the parental BT-549 cells and BT-Gal3 cells which grow as branched or stellate colonies as previously shown [21,22], BT-A6A cells grew as spherical colonies similar to MCF-10A acini [19]. This confirmed that depletion of AnxA6 in BT-549 cells promoted anchorage-independent cell growth but also abolished their invasiveness at least in vitro (Fig. 5B, cf. BT-549 and BT-A6A).

To ascertain whether AnxA6 depletion affected cellular motility and invasiveness, cells were seeded in thin membrane cell culture inserts with or without a thin layer of matrigel using complete DMEM/F12 (10% FBS) as the chemoattractant. Fig. 5C shows that BT-A6A cells exhibited reduced (at least 20 fold) motility compared to the parental BT-549 cells. As expected, MCF-10A cells were negligibly motile while the BT-Gal3 cells were about 5-fold less motile than the parental cells (Fig. 5C). Analysis of the invasive potentials of these cells revealed that BT-A6A cells were again at least 8-fold less invasive while the BT-Gal3 cells were slightly more invasive than the parental BT-549 cells (Fig. 5D). Together, this suggests that AnxA6 expression is necessary for the motile/invasive phenotype of breast cancer cells

and that the over-expression of N-cadherin, AnxA2 or AnxA4 (Fig. 2) was not sufficient to rescue the cells from the loss of AnxA6.

AnxA6 expression is important for the localization of focal adhesions at appropriate plasma membrane sites

From the preceding observations, we speculated that AnxA6 might affect the formation and/or maturation of adherens junctions and adhesion plaques at cell-cell and cell-ECM contact sites respectively. We first, examined the formation of these structures by immunofluorescence staining of vinculin in parental cells cultivated at various Ca^{2+} concentrations. Fig. 6A shows that parental BT-549 cells respond to an increase in extracellular Ca^{2+} by forming larger and more conspicuous adhesion plaques (arrow heads). To examine whether the reduced adhesion and motility of BT-A6A cells could be due to defective formation, localization and/or distribution of adhesion plaques, serum-starved cells were briefly treated with 2 mM Ca^{2+} and processed for visualization of vinculin-based adhesion plaques. As shown in Fig. 6B (arrow heads), the adhesion plaques in the parental BT-549 cells are conspicuous and peripherally located. In the spindle-shaped AnxA6-depleted cells these structures are not only fewer but are elongated, randomly distributed and concentrated at the tips of the cells (Fig. 6B, lower panel). A closer examination of the distribution of adhesion plaques at intercellular junctions (Fig. 6C, insets) in cells grown on glass cover slips in complete DMEM/F12 medium revealed discernible vinculin staining at intercellular junctions in the parental BT-549 cells (Fig. 6C, left panel). However, in BTA6A cells, the cell-cell contacts are not clearly demarcated by the vinculin structures (Fig. 6C, right panel). Together with data in Figs. 3, 4 and 5 this confirms that AnxA6 expression is required for the establishment of cell-cell cohesion as well as for cell-ECM interactions which are necessary for efficient motility and invasiveness of cancer cells.

The Ca^{2+}-dependent formation of adhesion plaques in BT-549 cells as shown in Fig. 6A prompted us to question whether the diminished cellular adhesion and motility following AnxA6 depletion could be due to defects in the generation of signals from focal adhesions. As shown in Fig. 7A, in the parental BT-549 cells and as expected, extracellular Ca^{2+} promoted the translocation of AnxA6 to membranes. To correlate the Ca^{2+}-dependent formation of both adhesion plaques (Fig. 6A) and AnxA6 translocation to membranes with the activity of focal adhesion kinase (FAK) known to be recruited to focal contacts, we investigated the effect of Ca^{2+} concentration on the autophosphorylation of FAK (phospho-Y397) in the parental BT-549 cells. Fig. 7B shows that the activation of FAK is indeed Ca^{2+}-dependent; FAK autotophosphorylation is at least 3-fold at 5 mM Ca^{2+} compared to Ca^{2+}-free conditions. We next, examined the effect of AnxA6 depletion on extracellular Ca^{2+}-dependent activation of FAK, and the downstream signaling cascades involving PI3 kinase and MAP kinase pathways [26]. To do this parental BT-549 and BT-A6A cells were treated with or without the indicated concentrations of Ca^{2+} for 10 min and the autophosphorylation of FAK or the activation of Akt (phospho-S473) and ERK1/2 (phospho-ERK1/2) were examined by western blotting in the respective cell lysates. We show that the activation of ERK1/2 is Ca^{2+}-dependent in the parental BT-549 cells. On the contrary, in BT-A6A cells the activity of ERK1/2 is not responsive to Ca^{2+} (Fig. 7C and D). As depicted in Fig. 7C we consistently observed at least 2-fold up-regulation of the total ERK2 levels. While, the activation of FAK in parental BT-549 cells is Ca^{2+}-dependent, it is strongly inhibited in BT-A6A cells (Fig 7C and E). We also observed that while PI3 kinase (depicted by phosphorylation of protein kinase B/Akt on S473) is activated in the parental BT-549 cells but its activation in BT-A6A cells is also strongly inhibited (Fig 7C and F). Together with data in figure 3, this suggests that the enhanced anchorage-independent proliferation of AnxA6-depleted cells is dependent on the constitutive activation of the Ras-Raf-MAP kinase pathway while AnxA6-dependent cellular adhesion and motility to a large

extent appears to be modulated via the formation and appropriate localization of functional focal adhesions and the activation of the FAK-PI3 kinase/Akt pathway.

AnxA6 expression is critical during the invasive stages of breast cancer

Our data on the growth of BT-A6A cells in 2D and 3D cultures (Figs. 3 and 5) revealed that AnxA6 is necessary for cell-cell cohesion and cell motility/invasiveness but its diminished expression promotes anchorage-independent cell proliferation. To correlate this with AnxA6 expression in breast cancer tissues, we examined its expression levels as well as the proliferative potential of cells in paraffin-embedded, formalin-fixed normal breast, invasive ductal carcinoma and in mucous adenocarcinoma human breast tissues (US-Biomax Inc.). We show that AnxA6 expression is strongest in the ductal epithelial cells in normal mammary tissues; it is however, decreased to about 60% in invasive ductal carcinoma tissues and even more so (about 10%) in mucous adenocarcinoma tissues (Fig. 8A, upper panel and Fig. 8B). The immunohistochemical staining of PCNA revealed that while cell proliferation is barely detected in normal breast tissues, we observe more active proliferation in the invasive ductal carcinoma tissues (scored as 100%) and about 60% proliferation in mucous adenocarcinoma tissues (Fig. 8A, lower panel and Fig. 8B). Fig. 8C confirms that unlike MCF-10A, primary mammary epithelial cells (HuMEC) are AnxA6-positive. Expression of vinculin was not significantly different in the parental and AnxA6-depleted BT-549 cells. Together, this demonstrates that although AnxA6 expression is reduced in breast cancer tissues, it remains relatively elevated in the invasive phenotype of breast cancer.

Discussion

Earlier studies in our and other laboratories revealed that AnxA6 is a candidate receptor for fetuin-A on the surface of breast cancer cells [20] and for chondroitin sulfate proteoglycans in several cell types [27]. Since these extracellular AnxA6-interacting partners are potential cell adhesion molecules, AnxA6 may mediate the interaction of cells with these ECM components. On the other hand, the stabilization of the cortical actin cytoskeleton following constitutive membrane targeting of AnxA6 [11] emphasizes the role of AnxA6 in cellular processes such as cell adhesion to the ECM and motility and perhaps their metastatic potentials. Another report that depletion of AnxA6 in the invasive MDA-MB-436 breast cancer cells promoted anchorage-independent cell proliferation [15] suggested yet another notion that AnxA6 might function as a tumor suppressor in breast cancer. The impetus for the present studies was therefore to address in greater detail this dichotomy in the role(s) of AnxA6 in breast cancer progression. Our data demonstrate that reduced AnxA6 expression contributes to breast cancer progression by promoting the loss of functional cell-cell and/or cell-ECM contacts and therefore enhanced anchorage-independent cell proliferation, presumably driven by sustained MAP kinase activation. Meanwhile, AnxA6-dependent cellular adhesion/motility may be driven by the PI3 kinase/Akt pathway due to the formation of functional focal adhesions at defined plasma membrane sites.

Annexins are known to be intracellular proteins which efficiently interact with biological membranes. However, several proteomic studies have consistently identified AnxA2 and AnxA6 in cell-derived exosomes [12,28,29] and on the surface of some cell types [16,27,30,31]. It is believed that annexins reach the cell surface by translocating from the inner leaflet to the extracellular face of the plasma membrane [32]. There is also sufficient evidence that these signal peptide-less proteins associate with nanovesicles or multi-vesicular bodies and are released as exosomes [33,34]. Our data show that these annexins are secreted by breast cancer cells via the exosomal pathway and that the secreted proteins are predominantly cell surface-associated. This more or less constitutive cell-surface association is supported by the fact that even at physiological Ca^{2+} concentrations (1.1-1.3

mM) extracellular annexins will almost entirely be membrane bound [4]. The quantitative difference between cell surface expression of AnxA2 and AnxA6 in BT-549 and other cell types [35] is not surprising because individual annexins require different Ca^{2+} concentrations for translocation to membranes [4,36] and/or subsequent secretion in exosomes.

Cell adhesion requires the interaction of cell surface receptors with their ECM ligands, followed by the clustering of adhesion receptors (cell spreading) and eventually the formation of adhesion plaques and actin stress fibers [37]. Extracellular AnxA6 may influence this process through its interaction with extracellular ligands including the serum glycoprotein fetuin-A, chondroitin sulfate containing proteoglycans [20,27] and as shown in this study, with the basement membrane collagen type IV. This receptor-ligand notion is supported by the demonstration that AnxA2 is the receptor for the matricellular protein tenascin-C [38] as well as plasmin and tissue plasminogen activator [35]. The interaction of AnxA2 with these ligands has been shown to affect cellular adhesion and migration [37,39]. The interesting observation that AnxA6 might mediate the interaction of breast cancer cells with the basement membrane collagen type IV is indicative of a potential role of AnxA6 as a metastasis-promoting factor. If this is true, then AnxA6 may play an important role during the migration of invasive cancer cells into and out of the vasculature by enhancing the interaction of tumor cells with the basement membranes of the endothelium.

The previous observation that AnxA6 expression is associated with divalent cation-dependent endothelial cell adhesion of metastatic RAW117 large-cell lymphoma cells [40] suggests that cell surface AnxA6 may directly mediate celI-cell interactions. In support of this putative function, annexins have been shown to self-aggregate on membrane surfaces in a Ca^{2+}-dependent manner [41]. This possibly occurs via the formation of “annexin bridges” between adjacent cells via their conserved domains [42]. It is possible that AnxA6 with two sets of 4 annexin repeats may be more efficient at forming such annexin bridges than either AnxA2 or other annexins with a single set of 4 annexin repeats. This again explains why in spite of over expression of AnxA2 and AnxA4 in AnxA6-depleted cells, the inhibition of cell-cell and cell-ECM interactions were not significantly overcome. This is supported by studies in which down regulation of AnxA1 [43,44], AnxA2 [39] or AnxA5 [45] in various cancer cell types influenced cell motility via distinct mechanisms and suggests that these proteins are not functionally redundant.

The motile phenotype of breast cancer cells is often associated with loss of E-cadherin and expression of N-cadherin [21,46]. The surprising observation that N-cadherin is up-regulated in the adhesion and motility-impaired AnxA6-depleted BT-549 cells support yet another idea that AnxA6 is required for cadherin function in cell-cell contacts. Although AnxA6 involvement remains to be verified, this possibility is consistent with a recent report in which AnxA2 was identified as a component of the vascular endothelial cell cadherin complex [47]. It is worth noting that over-expression of N-cadherin in motility-impaired cells has also been reported in LN18 glioblastoma cells following transfection with a dominant negative HER2 receptor variant [48].

Although other protein-AnxA6 interactions are possible, the demonstrated mode of association of AnxA6 with cell membranes is via membrane phospholipids [3]. As such AnxA6 participates in the formation of membrane-cytoskeleton complexes [36] and in a Ca^{2+}-dependent manner [4]. It should be recalled that focal contacts are actin-anchoring sites and recent studies confirmed that AnxA6 stabilizes the cortical actin cytoskeleton [11]. This supports the notion that like extracellular AnxA6 discussed above, intracellular AnxA6 also acts as a link between the plasma membrane and the cortical actin cytoskeleton. Therefore, although we could not demonstrate the presence of AnxA6 in focal contacts, it is

possible that AnxA6 indirectly stabilizes focal contacts at appropriate plasma membrane locations via its interaction with F-actin. It is also likely that AnxA6 does not influence the formation of vinculin-based focal contacts per se, but loss of AnxA6 expression may prevent the anchoring of these structures at appropriate locations in the plasma membrane. The requirement of AnxA6 in this process is supported by the altered cellular morphology as well as the elongated structure and dispersed localization of adhesion plaques following AnxA6 depletion in BT-549 cells.

This study enhances our understanding of two potential roles of AnxA6 in breast cancer progression viz. as a tumor suppressor and as a motility promoting factor. From our data it appears that in breast cancer, AnxA6 expression reduces as the disease progresses. Loss of AnxA6 has been linked with inhibition of store-operated Ca^{2+} entry [11], impaired membrane targeting of p120GAP which negatively regulates Ras activity [49] and therefore, sustained activation of the Ras-Raf-MAP kinase pathway. This sustained activation of the MAP kinase pathway appears to be a major contributing factor in enhanced anchorage-independent proliferation of AnxA6-depleted cells and therefore, enhanced tumor growth. Cell adhesion and motility/invasion on the other hand depend upon efficient reorganization of the cytoskeleton and more precisely on the propensity for rapid assembly and disassembly of cell-cell [50,51] and cell-ECM contacts [52]. This has been shown to be driven by the FAK-dependent activation of the PI3 kinase/Akt pathway [53]. Our data also reveal that the underlying cause for the inhibition of adhesion-related properties of AnxA6-depleted BT-549 cells is the inappropriate localization and/or functional integrity of focal contacts at sites of contact with the ECM and/or between cells. The defective focal contacts and the strong inhibition of the PI3 kinase/Akt pathway suggest that AnxA6-dependent adhesion and motility of invasive breast cancer cells rely on the activation of the FAK-PI3 kinase/Akt pathway. Therefore, while reduced AnxA6 expression is necessary for enhanced tumor growth via anchorage-independent cell proliferation, AnxA6 expression is required for cellular adhesion, motility and invasiveness.

Supplementary Material

Refer to Web version on PubMed Central for supplementary material.

Acknowledgments

This work was supported by grants from the NIH-NCI-Score 1 SC1 CA134018-01 (J.O); DOD W81XWH-07-1-0254 (J.O) and by NIH/NCRR/RCMI Grant Number 2G12RR003032-22.

References

1. Adams JC. Cell-matrix contact structures. Cell Mol Life Sci 2001;58:371–392. [PubMed: 11315186]
2. Pollard TD, Cooper JA. Actin, a central player in cell shape and movement. Science 2009;326:1208–1212. [PubMed: 19965462]
3. Gerke V, Creutz CE, Moss SE. Annexins: linking Ca2+ signalling to membrane dynamics. Nat Rev Mol Cell Biol 2005;6:449–461. [PubMed: 15928709]
4. Draeger A, Wray S, Babiychuk EB. Domain architecture of the smooth-muscle plasma membrane: regulation by annexins. Biochem J 2005;387:309–314. [PubMed: 15537390]
5. Sjolin C, Stendahl O, Dahlgren C. Calcium-induced translocation of annexins to subcellular organelles of human neutrophils. Biochem J 1994;300(Pt 2):325–330. [PubMed: 8002935]
6. Hayes MJ, Shao D, Bailly M, Moss SE. Regulation of actin dynamics by annexin 2. EMBO J 2006;25:1816–1826. [PubMed: 16601677]
7. Grewal T, Enrich C. Annexins--modulators of EGF receptor signalling and trafficking. Cell Signal 2009;21:847–858. [PubMed: 19385045]

8. Mussunoor S, Murray GI. The role of annexins in tumour development and progression. J Pathol 2008;216:131–140. [PubMed: 18698663]
9. Gerke V, Moss SE. Annexins: from structure to function. Physiol Rev 2002;82:331–371. [PubMed: 11917092]
10. Buzhynskyy N, Golczak M, Lai-Kee-Him J, Lambert O, Tessier B, Gounou C, Berat R, Simon A, Granier T, Chevalier JM, Mazeres S, Bandorowicz-Pikula J, Pikula S, Brisson AR. Annexin-A6 presents two modes of association with phospholipid membranes. A combined QCM-D, AFM and cryo-TEM study. J Struct Biol 2009;168:107–116. [PubMed: 19306927]
11. Monastyrskaya K, Babiychuk EB, Hostettler A, Wood P, Grewal T, Draeger A. Plasma membrane-associated annexin A6 reduces Ca2+ entry by stabilizing the cortical actin cytoskeleton. J Biol Chem 2009;284:17227–17242. [PubMed: 19386597]
12. Theobald J, Smith PD, Jacob SM, Moss SE. Expression of annexin VI in A431 carcinoma cells suppresses proliferation: a possible role for annexin VI in cell growth regulation. Biochim Biophys Acta 1994;1223:383–390. [PubMed: 7918674]
13. Smith DL, Evans CA, Pierce A, Gaskell SJ, Whetton AD. Changes in the proteome associated with the action of Bcr-Abl tyrosine kinase are not related to transcriptional regulation. Mol Cell Proteomics 2002;1:876–884. [PubMed: 12488463]
14. Francia G, Mitchell SD, Moss SE, Hanby AM, Marshall JF, Hart IR. Identification by differential display of annexin-VI, a gene differentially expressed during melanoma progression. Cancer Res 1996;56:3855–3858. [PubMed: 8752144]
15. Vila de Muga S, Timpson P, Cubells L, Evans R, Hayes TE, Rentero C, Hegemann A, Reverter M, Leschner J, Pol A, Tebar F, Daly RJ, Enrich C, Grewal T. Annexin A6 inhibits Ras signalling in breast cancer cells. Oncogene 2009;28:363–377. [PubMed: 18850003]
16. Hajjar KA, Guevara CA, Lev E, Dowling K, Chacko J. Interaction of the fibrinolytic receptor, annexin II, with the endothelial cell surface. Essential role of endonexin repeat 2. J Biol Chem 1996;271:21652–21659. [PubMed: 8702954]
17. Ochieng J, Pratap S, Khatua AK, Sakwe AM. Anchorage-independent growth of breast carcinoma cells is mediated by serum exosomes. Exp Cell Res 2009;315:1875–1888. [PubMed: 19327352]
18. Fukazawa H, Mizuno S, Uehara Y. A microplate assay for quantitation of anchorage-independent growth of transformed cells. Anal Biochem 1995;228:83–90. [PubMed: 8572292]
19. Debnath J, Muthuswamy SK, Brugge JS. Morphogenesis and oncogenesis of MCF-10A mammary epithelial acini grown in three-dimensional basement membrane cultures. Methods 2003;30:256–268. [PubMed: 12798140]
20. Kundranda MN, Ray S, Saria M, Friedman D, Matrisian LM, Lukyanov P, Ochieng J. Annexins expressed on the cell surface serve as receptors for adhesion to immobilized fetuin-A. Biochim Biophys Acta 2004;1693:111–123. [PubMed: 15313013]
21. Nieman MT, Prudoff RS, Johnson KR, Wheelock MJ. N-cadherin promotes motility in human breast cancer cells regardless of their E-cadherin expression. J Cell Biol 1999;147:631–644. [PubMed: 10545506]
22. Zajchowski DA, Bartholdi MF, Gong Y, Webster L, Liu HL, Munishkin A, Beauheim C, Harvey S, Ethier SP, Johnson PH. Identification of gene expression profiles that predict the aggressive behavior of breast cancer cells. Cancer Res 2001;61:5168–5178. [PubMed: 11431356]
23. Zeller KS, Idevall-Hagren O, Stefansson A, Velling T, Jackson SP, Downward J, Tengholm A, Johansson S. PI3-kinase p110alpha mediates beta1 integrin-induced Akt activation and membrane protrusion during cell attachment and initial spreading. Cell Signal 2010;22:1838–1848. [PubMed: 20667469]
24. Sakwe AM, Koumangoye R, Goodwin SJ, Ochieng J. Fetuin-A (ahsg) is a major serum adhesive protein that mediates growth signaling in breast tumor cells. J Biol Chem. 2010
25. Warfield PR, Makker PN, Raz A, Ochieng J. Adhesion of human breast carcinoma to extracellular matrix proteins is modulated by galectin-3. Invasion Metastasis 1997;17:101–112. [PubMed: 9561029]
26. Zhang X, Lin M, van Golen KL, Yoshioka K, Itoh K, Yee D. Multiple signaling pathways are activated during insulin-like growth factor-I (IGF-I) stimulated breast cancer cell migration. Breast Cancer Res Treat 2005;93:159–168. [PubMed: 16187236]

27. Takagi H, Asano Y, Yamakawa N, Matsumoto I, Kimata K. Annexin 6 is a putative cell surface receptor for chondroitin sulfate chains. J Cell Sci 2002;115:3309–3318. [PubMed: 12140262]
28. Janiszewski M, Do Carmo AO, Pedro MA, Silva E, Knobel E, Laurindo FR. Platelet-derived exosomes of septic individuals possess proapoptotic NAD(P)H oxidase activity: A novel vascular redox pathway. Crit Care Med 2004;32:818–825. [PubMed: 15090968]
29. Staubach S, Razawi H, Hanisch FG. Proteomics of MUC1-containing lipid rafts from plasma membranes and exosomes of human breast carcinoma cells MCF-7. Proteomics 2009;9:2820–2835. [PubMed: 19415654]
30. Kumar V, Farell G, Deganello S, Lieske JC. Annexin II is present on renal epithelial cells and binds calcium oxalate monohydrate crystals. J Am Soc Nephrol 2003;14:289–297. [PubMed: 12538728]
31. Patchell BJ, Wojcik KR, Yang TL, White SR, Dorscheid DR. Glycosylation and annexin II cell surface translocation mediate airway epithelial wound repair. Am J Physiol Lung Cell Mol Physiol 2007;293:L354–363. [PubMed: 17513451]
32. Bode G, Luken A, Kerkhoff C, Roth J, Ludwig S, Nacken W. Interaction between S100A8/A9 and annexin A6 is involved in the calcium-induced cell surface exposition of S100A8/A9. J Biol Chem 2008;283:31776–31784. [PubMed: 18786929]
33. Denzer K, Kleijmeer MJ, Heijnen HF, Stoorvogel W, Geuze HJ. Exosome: from internal vesicle of the multivesicular body to intercellular signaling device. J Cell Sci 2000;113(Pt 19):3365–3374. [PubMed: 10984428]
34. Thery C, Zitvogel L, Amigorena S. Exosomes: composition, biogenesis and function. Nat Rev Immunol 2002;2:569–579. [PubMed: 12154376]
35. Hajjar KA, Jacovina AT, Chacko J. An endothelial cell receptor for plasminogen/tissue plasminogen activator. I. Identity with annexin II. J Biol Chem 1994;269:21191–21197. [PubMed: 8063740]
36. Babiychuk EB, Palstra RJ, Schaller J, Kampfer U, Draeger A. Annexin VI participates in the formation of a reversible, membrane-cytoskeleton complex in smooth muscle cells. J Biol Chem 1999;274:35191–35195. [PubMed: 10575003]
37. Murphy-Ullrich JE. The de-adhesive activity of matricellular proteins: is intermediate cell adhesion an adaptive state? J Clin Invest 2001;107:785–790. [PubMed: 11285293]
38. Chung CY, Murphy-Ullrich JE, Erickson HP. Mitogenesis, cell migration, and loss of focal adhesions induced by tenascin-C interacting with its cell surface receptor, annexin II. Mol Biol Cell 1996;7:883–892. [PubMed: 8816995]
39. Sharma M, Ownbey RT, Sharma MC. Breast cancer cell surface annexin II induces cell migration and neoangiogenesis via tPA dependent plasmin generation. Exp Mol Pathol 2010;88:278–286. [PubMed: 20079732]
40. Tressler RJ, Yeatman T, Nicolson GL. Extracellular annexin VI expression is associated with divalent cation-dependent endothelial cell adhesion of metastatic RAW117 large-cell lymphoma cells. Exp Cell Res 1994;215:395–400. [PubMed: 7982479]
41. Zaks WJ, Creutz CE. Ca(2+)-dependent annexin self-association on membrane surfaces. Biochemistry 1991;30:9607–9615. [PubMed: 1911746]
42. Ayala-Sanmartin J. Cholesterol enhances phospholipid binding and aggregation of annexins by their core domain. Biochem Biophys Res Commun 2001;283:72–79. [PubMed: 11322769]
43. de Graauw M, van Miltenburg MH, Schmidt MK, Pont C, Lalai R, Kartopawiro J, Pardali E, Le Devedec SE, Smit VT, van der Wal A, Van't Veer LJ, Cleton-Jansen AM, ten Dijke P, van de Water B. Annexin A1 regulates TGF-beta signaling and promotes metastasis formation of basal-like breast cancer cells. Proc Natl Acad Sci U S A 2010;107:6340–6345. [PubMed: 20308542]
44. Maschler S, Gebeshuber CA, Wiedemann EM, Alacakaptan M, Schreiber M, Custic I, Beug H. Annexin A1 attenuates EMT and metastatic potential in breast cancer. EMBO Mol Med 2010;2:401–414. [PubMed: 20821804]
45. Wehder L, Arndt S, Murzik U, Bosserhoff AK, Kob R, von Eggeling F, Melle C. Annexin A5 is involved in migration and invasion of oral carcinoma. Cell Cycle 2009;8:1552–1558. [PubMed: 19372761]

46. Cavallaro U. N-cadherin as an invasion promoter: a novel target for antitumor therapy? Curr Opin Investig Drugs 2004;5:1274–1278.

47. Heyraud S, Jaquinod M, Durmort C, Dambroise E, Concord E, Schaal JP, Huber P, Gulino-Debrac D. Contribution of annexin 2 to the architecture of mature endothelial adherens junctions. Mol Cell Biol 2008;28:1657–1668. [PubMed: 18160703]

48. Rappl A, Piontek G, Schlegel J. EGFR-dependent migration of glial cells is mediated by reorganisation of N-cadherin. J Cell Sci 2008;121:4089–4097. [PubMed: 19033391]

49. Grewal T, Evans R, Rentero C, Tebar F, Cubells L, de Diego I, Kirchhoff MF, Hughes WE, Heeren J, Rye KA, Rinninger F, Daly RJ, Pol A, Enrich C. Annexin A6 stimulates the membrane recruitment of p120GAP to modulate Ras and Raf-1 activity. Oncogene 2005;24:5809–5820. [PubMed: 15940262]

50. Hartsock A, Nelson WJ. Adherens and tight junctions: structure, function and connections to the actin cytoskeleton. Biochim Biophys Acta 2008;1778:660–669. [PubMed: 17854762]

51. Niessen CM, Gottardi CJ. Molecular components of the adherens junction. Biochim Biophys Acta 2008;1778:562–571. [PubMed: 18206110]

52. Arnaout MA, Goodman SL, Xiong JP. Structure and mechanics of integrin-based cell adhesion. Curr Opin Cell Biol 2007;19:495–507. [PubMed: 17928215]

53. Parsons JT, Martin KH, Slack JK, Taylor JM, Weed SA. Focal adhesion kinase: a regulator of focal adhesion dynamics and cell movement. Oncogene 2000;19:5606–5613. [PubMed: 11114741]

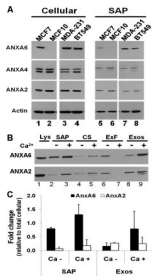

Figure 1. Secretion and association of annexins with the surface of breast carcinoma cells

A) The indicated breast cell lines were serum-starved for 24 h, then cultivated in HBSS containing 0.5 mM Mg^{2+} and 2 mM Ca^{2+} for 2 h at 37°C. Cells were washed twice with HBSS and the surface-associated proteins eluted in HBSS containing 10 mM EGTA. Equal amounts of proteins were dissociated and analyzed in 4-12% SDS gels and immunoblotting with the indicated antibodies. B) BT-549 cells were serum-starved, incubated in HBSS with or without 2 mM Ca^{2+}. The surface-associated proteins as well as the secreted proteins were prepared and fractionated as described in “materials and methods”. Equal amounts of the various fractions were analyzed by immunoblotting using antibodies to AnxA2 or AnxA6. C) Densitometric analysis of AnxA2 and AnxA6 in the EGTA-solubilized (SAP)and exosome-associated fractions (Exos). Bars represent relative amounts ± SD from three independent experiments of surface-associated AnxA2 or AnxA6 normalized to each protein in total cell lysates. Lys: total cell lysates; SAP: surface-associated proteins; CS: culture supernatants (secreted proteins).

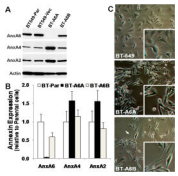

Figure 2. Down regulation of AnxA6 in BT-549 breast carcinoma cells

A) Parental BT-549 cells (BT-549-Par) were transfected with empty vector (BT-549-Vect) or small hairpin RNAs (A6A and A6B) targeting distinct regions of the coding sequence of AnxA6. Stable puromycin-selected clones were expanded and the extent of AnxA6 depletion assessed by immunoblotting (panel A) using antibodies against AnxA2, AnxA4 or AnxA6. Detection of β-actin in the cell lysates was used as the protein loading control. B) Densitometric analysis of annexin expression in AnxA6-depleted BT-549. Expression levels were normalized to β-actin. Bars represent annexin expression ± SD from three independent experiments relative to the expression level in the parental BT-549 cells. C) Changes in morphology following AnxA6 depletion in BT-549 cells. Equal number of cells were seeded in 12-well plates and cultivated in complete DMEM/F12. The morphology of parental BT-549 BT-A6A and BT-A6B cells was monitored microscopically.

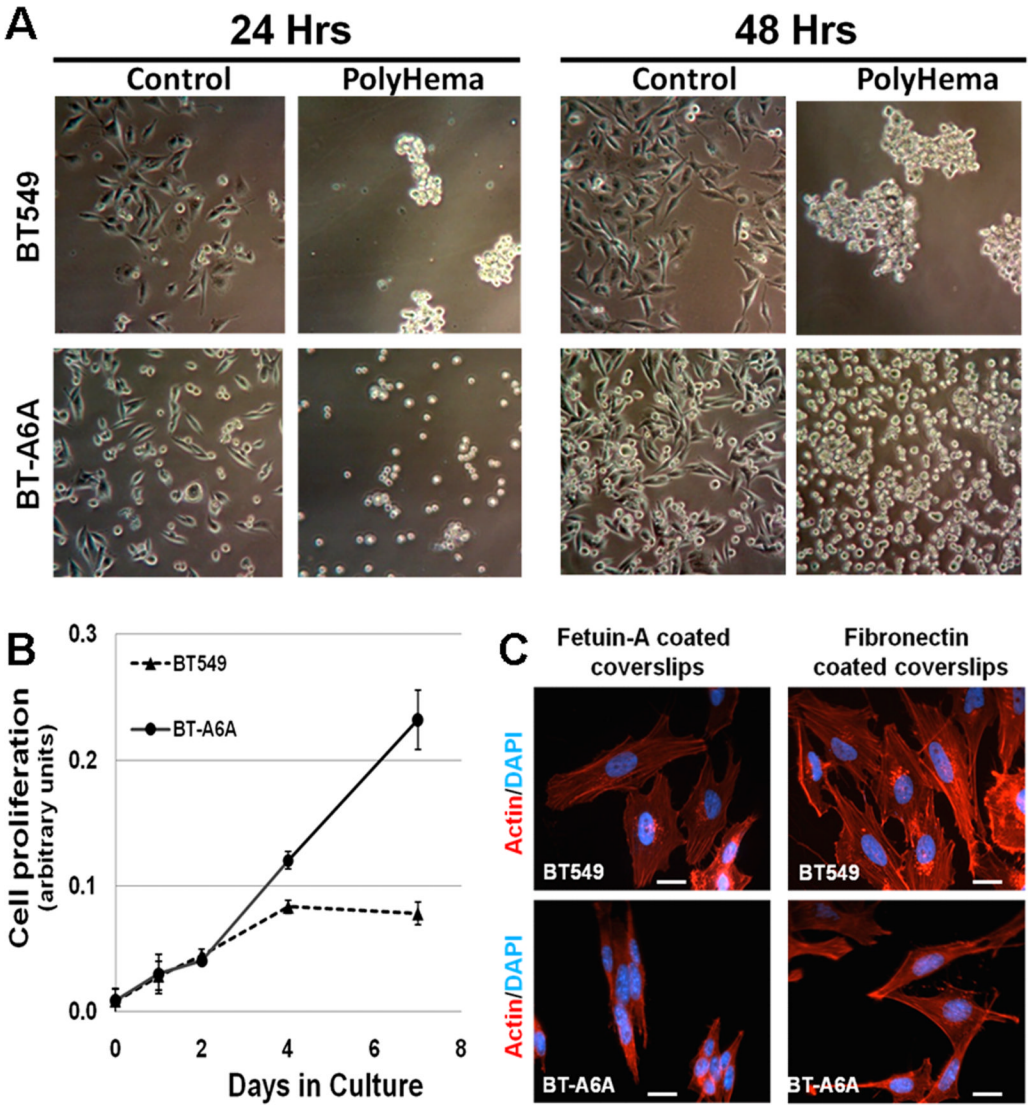

Figure 3. Anchorage-independent proliferation of AnxA6 depleted BT-549 cells

A) Parental BT-549 or BT-A6A cells were seeded (1×10^6) in complete DMEM/F12 medium in 100 mm dishes coated with or without polyHEMA. Growth of the cells was monitored microscopically (x10) 24 and 48 h later. B) Growth curves. Cells were plated in quadruplicate at 10^4 cells/well of a 24-well plate in complete DMEM/F12 medium. At the indicated time points, the proliferation of parental and BT-A6A cells was evaluated using the alamar blue colorimetric assay. C) Parental BT-549 or BT-A6A cells were grown on fetuin-A- or fibronectin-coated glass cover slips in serum-free medium for 24 h at 37 °C. Cells were washed with HBSS and promptly fixed in 3% PFA in PBS. The cells were then stained with rhodamine-labeled phalloidin and the cover slips mounted with Prolong Gold with DAPI. Bars = 10 μm.

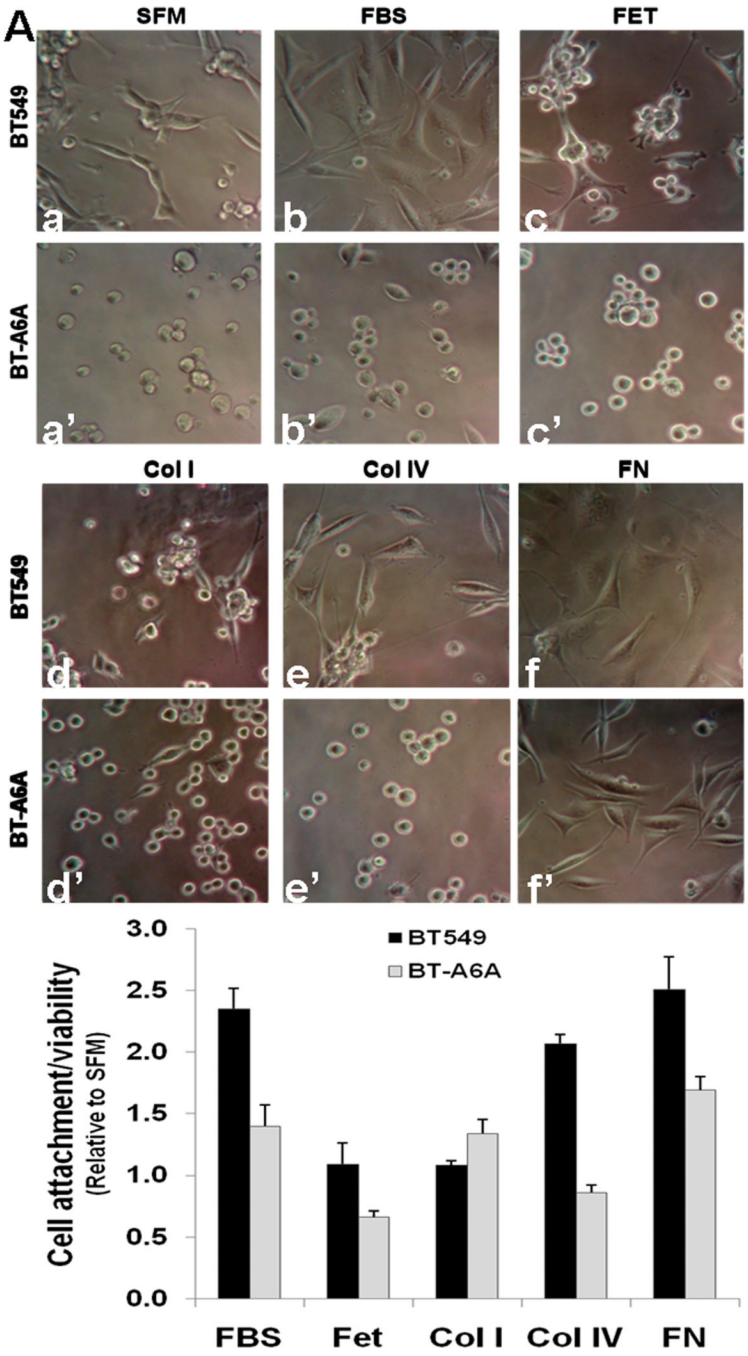

Figure 4. Adhesion/spreading of BT-A6A cells on fetuin-A or extracellular matrix components

A) Parental BT-549 or BT-A6A cells were harvested by treatment with 2 mM EDTA, washed abundantly in serum-free DMEM/F12 and seeded in triplicate at a concentration of 10^4 cells/well in serum-free medium (SFM, a and a'), complete DMEM/F12 (FBS, b and b') or in wells of a microtitre plate pre-coated with fetuin-A (FET, c and c'), collagen type I (Col I, d and d'), Collagen type IV (Col IV, e and e') or fibronectin (FN, f and f'). After incubation over-night at 37°C, 5% CO_2, the media and floating cells were aspirated and rinsed once with PBS. Cell adhesion/spreading were examined microscopically (x10). C) The number and viability of adherent cells estimated using the alamar blue colorimetric

assay. Bars represent cell adhesion and viability relative to serum-free medium ± SEM from three independent determinations.

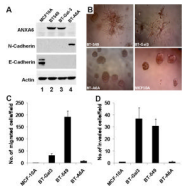

Figure 5. Effect of AnxA6-depletion on the growth in 3D cultures, motility and invasiveness of BT-549 cells

A) Total cell lysates were prepared from the indicated cell lines as described in "experimental procedures". Equal amounts of proteins were separated in 4-12% SDS gels and transferred to nitrocellulose membranes. The blots were probed with the indicated antibodies and revealed using enhanced chemiluminescence. B) Growth in 3D cultures on matrigel. Parental BT-549 or BT-A6A cells were harvested by trypsinization, rinsed and resuspended in complete DMEM/F12 medium at a concentration of 10^4 cells/ml. About 5×10^3 cells in complete DMEM/F12 were seeded on a layer of matrigel in a 96 well plate, and incubated at 37 °C for up to 10 days. The cells were photographed (x10) to determine the morphology of the colonies. C-D) Migration and invasion assays. Parental BT-549 or BT-A6A cells were harvested by trypsinization, washed abundantly in serum-free DMEM/F12 and resuspended in the same medium. About 2.5×10^5 cells in serum-free medium were plated in triplicate in the upper chambers of 8μm culture inserts (panel C) or the inserts containing a thin layer of matrigel (panel D) in 24 well plates. Complete DMEM/F12 as the chemoattractant was added to the lower chambers followed by incubation at 37°C for 24 h. After incubation, the media and floating cells in the upper insert chamber were aspirated and removed with cotton swab and the migrated cells fixed and stained with crystal violet. Migrated cells were photographed and counted. Bars represent the number of migrated cells/ field (C) or the number of cells that had invaded the matrigel/field (D) ± SD from three independent determinations.

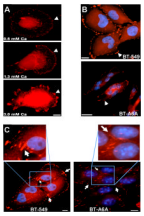

Figure 6. Altered morphology of focal contacts in BT-A6A cells

A) Ca^{2+}-dependent formation of adhesion plaques. Parental BT-549 cells were grown on glass cover slips in complete DMEM/F12 medium, then serum-starved overnight. The cells were subsequently washed twice in HBSS and then treated with the indicated concentrations of Ca^{2+} in HBSS for 60 min. The cells were then simultaneously fixed/ and permeabilized for 2 min in 3% PFA in PBS containing 0.5% Triton X-100. Adhesion plaques were stained with monoclonal antibodies to vinculin. B) Adhesion plaques in BT-A6A cells. BT-549 and BT-A6A cells were grown on glass cover slips in complete DMEM/F12 medium, fixed as in (A) above and adhesion plaques stained with antibodies to vinculin. C) Intercellular adhesion plaques. Cell were grown and processed as in (B) above. The inserts show vinculin staining at cell-cell junctions. Notice the conspicuous cell-cell contacts in the parental BT-549 cells and the virtual absence of these linkages between the BT-A6A cells. Bars = 10 μm

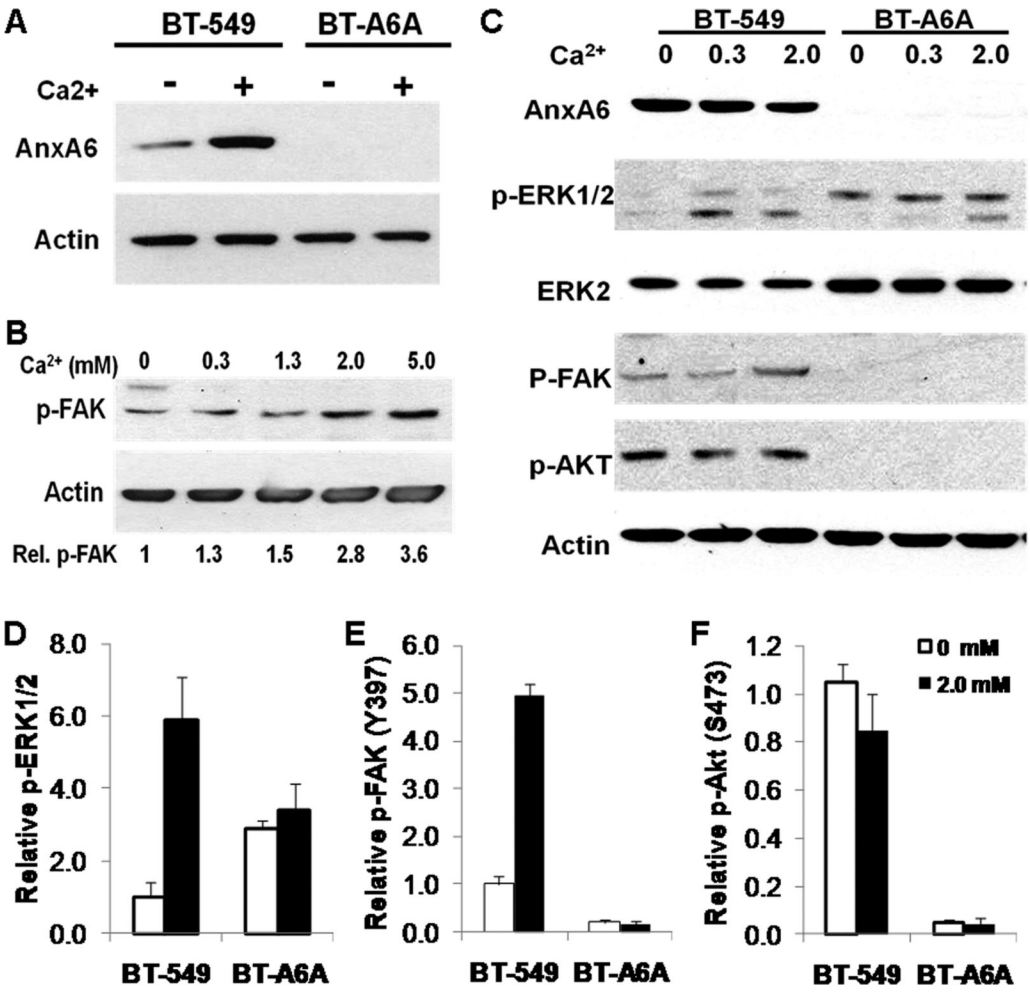

Figure 7. Extracellular Ca^{2+} signaling in BT-A6A breast carcinoma cells

BT-549 cells were seeded in complete DMEM/F12 medium, then serum-starved overnight. The cells were subsequently washed twice in HBSS and then treated with the indicated concentrations of Ca^{2+} in HBSS for 15 min. Crude membrane proteins and total cell lysates were prepared as described in "materials and methods" and equal amounts of protein used for analyses by immunoblotting. Blots were revealed using the enhanced chemiluminescence. A) Membrane translocation of AnxA6 was determined by western blotting of crude membrane extracts from BT-549 and BT-A6A cells using antibodies to AnxA6; detection of β-actin was used as the loading control. B) Autophosphorylation of focal adhesion kinase was examined by western blotting of total cell lysates of BT-549 cells cultivated at the indicated Ca^{2+} concentrations using antibody to phosphorylated FAK (Y397); detection of β-actin was used as the loading control. Fold change in p-FAK relative to cells in Ca^{2+}-free HBSS is indicated below each condition for this representative experiment. C) Activation of MAP kinase ERK1/2, PI3 kinase and FAK in total cell lysates were detected by immunoblotting using antibodies to phosphorylated ERK1/2, phosphorylated Akt(S473) and phosphorylated FAK(Y397) respectively; detection of total ERK2 or β-actin were used as the loading controls. D-F) Densitometric analyses of the activation of ERK1/2 (D), FAK (E) and PKB/Akt (F) in parental versus AnxA6-depleted BT-549 cells following treatment with or without 2mM Ca^{2+}. Activation of ERK1/2 was normalized to total ERK2, while activation of FAK and Akt were normalized to β-actin. Notice the at least two-fold increase in total ERK2 in BT-A6A cells. Bars represent fold

change in activation status ± SD compared to activity in parental BT-549 cells in Ca^{2+}-free conditions from three independent experiments.

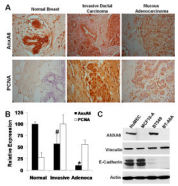

Figure 8. Expression of AnxA6 in breast cancer tissues

A) Thin sections of normal breast, invasive ductal carcinoma or mucous adenocarcinoma tissues were stained with antibodies to AnxA6 or the proliferating cell marker PCNA and counterstained with hematoxylin. All images are x40. B) Densitometric analysis of the stained sections from normal breast (normal); invasive ductal adenocarcinoma (invasive) and mucous adenocarcinoma (Adenoca) tissues. Bars indicate staining intensity relative to maximum staining from four random sections. Statistical analysis was performed using the Student's t-test; (#) $p < 0.05$; (*) $p < 0.0002$. C) Expression of annexin A6 in primary human mammary epithelial cells. Total cell lysates were prepared from the indicated cell lines or HuMECs as described in “materials and methods”. Equal amounts of proteins were separated in 4-12% SDS gels, transferred to nitrocellulose membranes and the blots probed with the indicated antibodies. Blots were revealed using enhanced chemiluminescence.